ELSEVIER

Journal of Fluids and Structures 24 (2008) 467–480

JOURNAL OF FLUIDS AND STRUCTURES

www.elsevier.com/locate/jfs

Two-dimensionality of a cantilevered-cylinder wake in the presence of an oscillating upstream cylinder

S.J. Xu[a], Y. Zhou[b,*], J.Y. Tu[c]

[a]*School of Aerospace, Tsinghua University, Beijing 100084, PR China*
[b]*Mechanical Engineering Department, Hong Kong Polytechnic University, Hung Hom, Kowloon, Hong Kong*
[c]*School of Aerospace, Mechanical and Manufacturing Engineering, RMIT University, VIC 3083, Australia*

Received 2 February 2007; accepted 21 October 2007
Available online 21 February 2008

Abstract

The effect of a longitudinally oscillating cylinder on the two-dimensionality of flow around a downstream cylinder is studied based on a two-point correlation measured using two hot-wires. The oscillation amplitude is $A/d = 0.472$ and the oscillation frequency $f_e/f_s = 0.0372$ and 0.186, where d is the cylinder diameter and f_s the frequency of natural vortex shedding from an isolated stationary cylinder. Three centre-to-centre spacing (L) ratios of the two cylinders were examined, i.e., $L/d = 1.8$, 2.5 and 4.8, representing three typical flow regimes. The experiment was conducted at a Reynolds number (Re) of 5920, based on d and the free-stream velocity. It is found that the spanwise correlation of the flow depends on not only the oscillation but also the flow regimes. At $L/d = 1.8$, the correlation is strongest among the three regimes, but worst in the co-shedding regime ($L/d = 4.8$). The upstream cylinder oscillation improves the spanwise correlation of the flow in the gap of the cylinders, irrespective of regimes, especially for $L/d = 1.8$ and 2.5, but impairs that behind the cylinders for $L/d = 1.8$ and 2.5 due to a change in the flow regime. A theoretical analysis based on the boundary vorticity theory indicates that the oscillation increases the vorticity flux, in particular, in the spanwise direction between the cylinders, resulting in a significantly improved spanwise correlation, though this increase is negligibly small behind the downstream cylinder.

1. Introduction

Flow past a cylinder of finite length can statistically be three-dimensional (3-D), due to the effect of end conditions [e.g., Szepessy and Bearman (1992)], as reflected by the varying spanwise correlation coefficients between simultaneously measured two-point velocity, surface pressure or sectional lift force [e.g., Ribeiro (1992), Szepessy (1994), Norberg (2003)]. The knowledge of the two-dimensionality of a flow is important not only fundamentally but also practically. For example, this knowledge is essential for the choice of spanwise numerical resolution in a simulation (Lucor et al., 2003); for a strongly three-dimensional flow, the mesh in the spanwise direction must be refined.

It has been well established that the two-dimensionality of flow around an oscillating cylinder can be substantially enhanced by the occurrence of the so-called 'lock-on' phenomenon; that is, when the cylinder oscillating frequency f_e approaches the natural vortex shedding frequency (f_s) of a stationary cylinder, the vortex shedding frequency was modified by f_e so that the two frequencies coincide with each other (Bishop and Hassan, 1964). Koopmann (1967) and

*Corresponding author. Tel.: +852 2766 6662.
E-mail address: mmyzhou@polyu.edu.hk (Y. Zhou).

0889-9746/$ - see front matter © 2007 Elsevier Ltd. All rights reserved.
doi:10.1016/j.jfluidstructs.2007.10.006

Toebes (1969) reported the increased spanwise coherence of vortex shedding of an elastic cylinder in the lock-on state ($Re < 300$). Koopmann's (1967) flow visualization photographs clearly showed that vortex shedding was in phase with the vibration of the cylinder when the cylinder lateral amplitude ratio, A/d, was above a threshold of 0.1. Ramberg and Griffin (1976) measured the spanwise correlation coefficient (R_{uu}) of fluctuating velocities along a forced vibrating cable ($A/d = 0.13$–0.3) at the onset of lock-on for $Re = 400$–1300. The measured R_{uu} surprisingly approached unity. Blackburn and Melbourne (1997) noted that the spanwise correlation length based on the lift measurements of a laterally oscillating cylinder shrank greatly with an increased longitudinal turbulence.

In engineering, multiple vibrating slender structures are frequently seen. Naturally, investigations have been extended to a cylinder wake in the presence of a neighbouring cylinder. There have been few reports of spanwise correlation near each of two tandem cylinders. Based on surface pressure measurements on two tandem cylinders, Arie et al. (1983) examined the effect of the cylinder centre-to-centre spacing L/d on the spanwise correlation length $L_z(\theta)$, defined as $L_{pz}(\theta) = \int_0^\infty R_{pp}(\theta, z)\,dz$ measured at $Re = 2.2$–4.4×10^4 and $L/d = 2$–10, where θ is an angle from the leading stagnation line and R_{pp} is the spanwise correlation between pressure signals. They found that L_{pz} reached a maximum at $L/d = 2$ at the separation region of the downstream cylinder, that is, $\theta = 90$–110°. Furthermore, L_{pz} for the upstream cylinder grew as L/d increased from $L/d = 2$ to 4 but diminished for $L/d = 4$–5, and then remained almost constant for $L/d > 5$. In contrast, L_{pz} for the downstream cylinder shrank rapidly from $L/d = 2$ to 4 but slowly for $L/d > 4$. Wu et al. (1994) obtained the spanwise coherence of two tandem cylinders with an aspect ratio of 23.6, fitted with end plates, using two hot-wires for $L/d = 3$–12 and $Re = 1.7 \times 10^4$–4.2×10^4. They found that the spanwise coherence at the vortex-shedding frequency decreased for $L/d > 4$. For $L/d = 3$ and 4, the coherence of the same spanwise separation measured behind the cylinders ($x/d = 5.5$) exceeded that of a single cylinder. This coherence furthermore was substantially larger at $L/d = 3$ than those at $L/d \geqslant 4$ between the cylinders ($x/d = -1.6$, where the origin of the coordinate system is defined at the centre of the downstream cylinder). The streamwise vortex, they observed, was considered to be largely responsible for the three-dimensionality of the flow.

Lai et al. (2003) examined the effect of an oscillating cylinder on a neighbouring side-by-side-arranged cylinder and found that the oscillating cylinder could lock-on to the vortex shedding frequency from the neighbouring cylinder as well as from itself. This finding implies that an oscillating cylinder may have an impact upon the two-dimensionality of a neighbouring cylinder wake. This aspect has not been well documented in the literature. Furthermore, previous studies mostly focused on the lock-on cases. For instance, Mahir and Rockwell (1996a, b) investigated flow ($Re = 160$) around two transversely in phase or in antiphase oscillating cylinders arranged in tandem and side-by-side, respectively. Their nominal cylinder centre-to-centre spacing was 2.5 and 5.0, respectively. The cylinder aspect ratio was 108 and presumably the end effect was negligibly small. There have been few investigations on the nonlock-on cases, which are commonly seen in engineering. The issues motivate the present investigation.

This work aims to investigate the possible effect an oscillating cylinder may have on the two-dimensionality of flow around a downstream cylinder and the dependence of this effect on the cylinder centre-to-centre spacing ratio L/d. The oscillation is not locked on with the frequency of vortex shedding from neither the upstream nor the downstream cylinder. Furthermore, the end effect was considered. Experimental details are described in Section 2. The results and discussion of the spanwise correlation coefficient obtained from hot-wire measurements between and behind the two cylinders are presented in Sections 3 and 4. The work is summarized in Section 5.

2. Experimental details

Experiments were carried out in a closed-loop wind tunnel with a 2.4 m long square working section (0.6 m × 0.6 m). The wind speed in the working section can be adjusted from about 0.3–50 m/s. More details of the tunnel were described in Zhou et al. (2002) and Huang et al. (2006). Two aluminium alloy circular cylinders of the same diameter $d = 0.0127$ m were cantilever-mounted in tandem in the horizontal mid-plane of the working section (Fig. 1). No end-plates were mounted. The upstream cylinder was placed 0.2 m downstream of the exit plane of the tunnel contraction. The aspect ratio of the cylinders was 17, causing a blockage of 2.1%. Three cylinder centre-to-centre spacings, i.e., $L/d = 1.8$, 2.5 and 4.8, were investigated, each representing one of the three flow regimes of two tandem stationary cylinders as classified by Zdravkovich (1987). The upstream cylinder was driven to oscillate harmonically in the streamwise direction by a computer-controlled motor system, which allowed the accurate adjustment of the oscillation frequency and amplitude. Experiments were conducted at $Re\ (\equiv U_\infty d/\nu) = 5920$ with and without the upstream cylinder oscillating, where U_∞ is the free-stream velocity, and ν is the kinematic viscosity of fluid. The oscillation amplitude and frequency were fixed at $A/d = 0.472$, and $f_e/f_s = 0.0372$ and 0.186, respectively, where f_s is the natural vortex shedding frequency of a stationary cylinder. The choice of the oscillation frequencies is two-fold. Firstly, this is a typical nonlock-on case. Secondly, based on the nonlinear theory, the superharmonic resonance may occur in applications (Nayfeh and Mook, 1979), and it would be interesting to examine

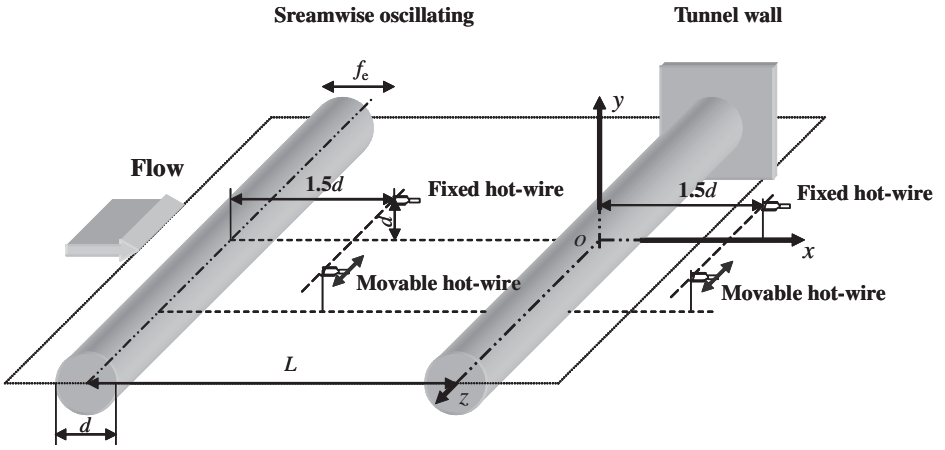

Fig. 1. Schematic of experimental set-up. The hot-wires were placed at $y/d = 1$ and $x/d = 1.5$ when measuring the flow behind the downstream cylinder or—$L/d + 1.5$ when measuring the flow between the cylinders.

the influence of the superharmonic resonance on the downstream cylinder wake. This potential influence may have applications in flow control, where the input energy is preferably small, that is, the oscillation frequency should be much smaller than the natural vortex shedding frequency at a given oscillation amplitude. For the purpose of comparison, measurements were also conducted around two tandem stationary cylinders ($d = 0.0127$ m), which spanned the full width of the working section, giving an aspect ratio of about 47.

It is worth commenting on the relatively short aspect ratio (17) of the cylinders. It is well known that a stationary cylinder may be subjected to end effects if its aspect ratio is below 27–30 (King, 1977). However, the flow two-dimensionality may be significantly improved if the cylinder is forced to oscillate. Griffin (1980) observed that, for a large aspect ratio cylinder (>30), when the oscillation amplitude ratio A/d was greater than 0.01–0.02, the correlation coefficient, R_{pp}, between spanwise fluctuating pressures increased greatly, compared with a stationary cylinder. Given a threshold of $R_{pp} = 0.5$, the spanwise correlation length was $10d$ at $A/d = 0.125$ but became $34d$ for $A/d = 0.472$ (the present oscillation amplitude) based on an extrapolation of his data. Xu et al. (2006) examined the flow around a streamwise oscillating cylinder of the same aspect ratio (17) and confirmed the reasonably two-dimensional flow around the cylinder. How the oscillation would impact upon a downstream cylinder of the same aspect ratio is an issue to be clarified in this work.

The coordinate system (x, y, z) is defined in Fig. 1; the fluctuating velocities and vorticity components along the three directions are denoted by (u, v, w) and (ω_x, ω_y, ω_z), respectively. Two single hot-wires, placed at $y/d = 1$, $x/d = (1.5 - L/d)$ and 1.5, were employed to measure simultaneously the longitudinal velocity fluctuation, $u(t)$, in the gap of and behind the two cylinders. One of the hot-wires was fixed at the mid-span of the cylinders and the other was movable along the spanwise direction of the cylinder. The movable hot-wire probe was mounted on a Dantec 3-D traversing mechanism controlled by a computer. The positioning resolution of the traversing mechanism was 0.05 mm. The sensing elements of the two wires, made of tungsten wire of 5 μm in diameter and approximately 3 mm in length, were operated on constant temperature circuits at an overheat ratio of 1.5. The signals from the hotwires were offset, amplified and then digitized at a sampling frequency $f_{\text{sample}} = 1.5$ kHz per channel using a 16 channel (12 bit) analog-to-digital board. The typical duration of each record was about 30 s.

The flow structure was visualized using Dantec Standard PIV 2100. The smoke was introduced from the upstream cylinder at mid-span. One NewWave standard pulsed laser source of a wavelength of 532 nm, having a maximum energy output of 120 mJ, was deployed to illuminate the smoke-seeded flow. The photographs of the flow were taken by a Hisence CCD digital camera with a resolution of 1280×1024 pixels. The framing rate is about 8 fps.

3. Experimental results

The spanwise correlation coefficient is defined (Zhou and Antonia, 1995) by

$$R_{uu}(\Delta z) = \frac{\overline{u_1(z,t)u_2(z+\Delta z,t)}}{\overline{u_1^2(z,t)}^{1/2}\overline{u_2^2(z+\Delta z,t)}^{1/2}}, \tag{1}$$

where u_1 and u_2 are the fluctuating velocity signals measured by the fixed and movable probes, respectively, with a spanwise separation of Δz (Fig. 1). The numerator in (1) represents the cross-correlation between u_1 and u_2, and the denominator is the product of the root mean square values of the two time series. For the purpose of comparison, a correlation length, L_{uu}, is defined as Δz, where $R_{uu}(\Delta z) = 0.5$. Since the results at $f_e/f_s = 0.186$ are qualitatively the same as at $f_e/f_s = 0.0372$, the latter only will be presented.

3.1. R_{uu} in the gap of the cylinders

Fig. 2 presents R_{uu} near the upstream cylinder at $L/d = 1.8$, 2.5 and 4.8, corresponding to the three different flow regimes, i.e., the single-body, reattachment and co-shedding regimes, in a two-tandem-stationary-cylinder wake (Igarashi, 1981; Zdravkovich, 1987; Xu and Zhou, 2004). The results of two stationary cylinders (aspect ratio = 47) are also included to provide a benchmark for comparison. As expected, the spanwise coherence for the stationary cylinders of large aspect ratio (= 47) is stronger than that for the stationary cylinders of small aspect ratio (= 17), since the end effect of the former on the flow is smaller than that of the latter. The correlation coefficient (R_{uu}) declines with increasing z/d for all cases. For the stationary cylinders of large aspect ratio, R_{uu} is not so much different from $L/d = 2.4$ to 4.8 but is considerably smaller at $L/d = 1.8$; L_{uu} is 3, 4.2 and 4.3 for $L/d = 1.8$, 2.5 and 4.8, respectively (Table 1). The shear layers separated from the upstream cylinder shoot over the downstream one at $L/d = 1.8$ but reattach on the downstream one at $L/d = 2.5$. At $L/d = 1.8$, R_{uu} obtained in the gap of the cylinders measures the spanwise correlation of the shear layers, not vortices. The fluid that occurs between the two shear layers separated from the upstream cylinder was observed in our flow visualization to move unsteadily along y and z directions, implying varying v and w and probably ω_x and ω_y, thus adversely affecting the spanwise correlation length of flow. At $L/d = 2.5$, L_{uu} increases significantly since the fluid movement occurring at $L/d = 1.8$ subsides greatly (not shown). The feedback response from the shear layer reattachment may reduce L_{uu}, though only slightly. At $L/d = 4.8$, vortex shedding from the upstream cylinder occurs, enhancing the two-dimensionality of the gap flow; the effect of both fluid movement at $L/d = 1.8$ and downstream feedback response is negligibly small. As the aspect ratio is reduced from 47 to 17, R_{uu} drops appreciably at $L/d = 1.8$ and 2.5 due to the increased flow three-dimensionality under the end effect; L_{uu} is 2.2 and 1.6 for $L/d = 1.8$ and 2.5, respectively. The most drastic drop in R_{uu} occurs at $L/d = 4.8$; L_{uu} is only 0.4. At $L/d = 1.8$, the shear layer around the cylinder free end overshoots the downstream cylinder end; the end condition has a weak effect on R_{uu} in the gap of two cylinders. As L/d increases, the shear layer around the cylinder free end reattaches the downstream cylinder end at $L/d = 2.5$ and even form vortices at $L/d = 4.8$. These vortices are highly

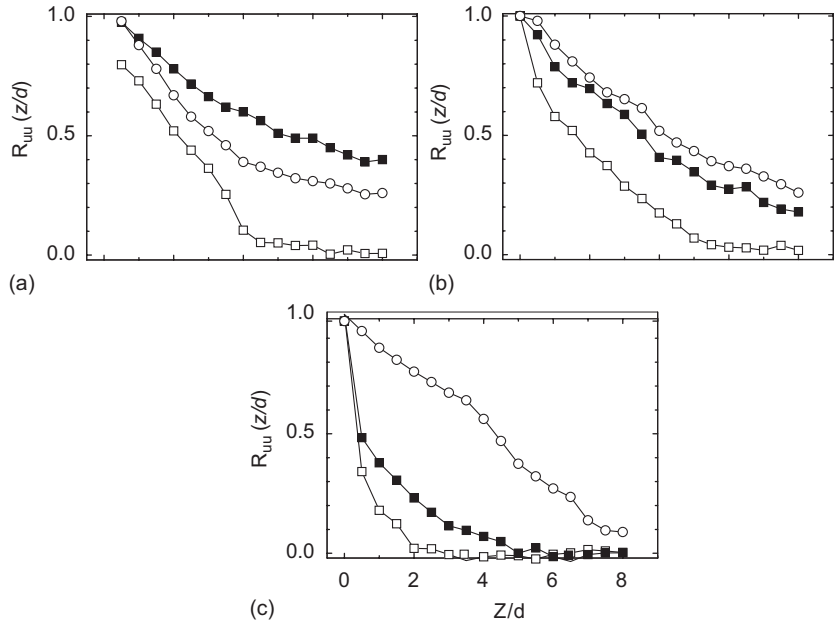

Fig. 2. Spanwise correlation coefficient, R_{uu}, of hot-wire signals measured between the cylinders at Re = 5920: (a) $L/d = 1.8$, (b) 2.5, and (c) 4.8. ■, Oscillation; □, without oscillation; ○, stationary cylinder with large-aspect-ratio of 47.

Table 1
Correlation length for each case

	L_{uu} between cylinders			L_{uu} behind cylinders		
	Aspect ratio = 47	Aspect ratio = 17		Aspect ratio = 47	Aspect ratio = 17	
L/d	Stationary	Stationary	Oscillation	Stationary	Stationary	Oscillation
1.8	3.0	2.2	5.2	4.0	4.2	3.3
2.5	4.2	1.6	3.5	3.8	1.3	2.5
4.8	4.3	0.4	0.6	0.8	0.5	0.5

three-dimensional, increasing the three-dimensionality of the flow away from the free end and contributing to the drop in L_{uu} between the cylinders.

In the presence of the cylinder oscillation, R_{uu} is greatly enhanced, L_{uu} increasing from 2.2 in the absence of oscillation to 5.2 for $L/d = 1.8$, 1.6 to 3.5 for $L/d = 2.5$, and 0.4 to 0.6 for $L/d = 4.8$. Its value (L_{uu}) exceeds considerably its counterpart of the stationary cylinders of large aspect ratio at $L/d = 1.8$ and is comparable at $L/d = 2.5$ (Figs. 2(a) and (b)). It may be concluded that the oscillation has significantly improved the flow two-dimensionality, similarly to an isolated cylinder case (Griffin, 1980).

3.2. R_{uu} behind the cylinders

Fig. 3 presents R_{uu} measured behind the downstream cylinder at $L/d = 1.8$, 2.5 and 4.8. Similarly to the flow in the gap of the two cylinders, R_{uu} decreases with increasing z/d. In the 'long' cylinder case (aspect ratio = 47), L_{uu} is about 4 and 3.8 (see Table 1) at $L/d = 1.8$ and 2.5, respectively, quite comparable to their counterparts in the gap of the two cylinders. This length is, however, only about 0.8 at $L/d = 4.8$, suggesting highly 3-D vortices. The observation is consistent with the report of Zhou and Yiu (2006) that vortices behind two tandem cylinders were very weak in the co-shedding regime. For the 'short' cylinder (aspect ratio = 17), L_{uu} is 4.2, 1.3 and 0.5 at $L/d = 1.8$, 2.5 and 4.8, respectively, showing little variation at $L/d = 1.8$ and 4.8 but by more than 65% at $L/d = 2.5$, compared with the 'long' cylinder. This variation is caused by a flow regime change at $L/d = 2.5$ since the aspect ratio changes from 47 to 17. The shear layers separating from the upstream cylinder reattach not only on both sides of the downstream cylinder but also on the downstream cylinder free end for the 'short' cylinder. In the latter situation, the shear layers re-separate from the edge of the cylinder end, generating ω_x and ω_y and enhancing the three-dimensionality of flow behind the cylinders. At $L/d = 1.8$, flow measured between the cylinders is much less coherent than behind; L_{uu} increases up to 91% (from 2.2 to 4.2), compared with that in the gap of the cylinders. From $L/d = 1.8$ to 4.8, L_{uu} drops, especially for the 'short' cylinders.

The upstream cylinder oscillation leads to a deteriorated spanwise correlation at $L/d = 1.8$ behind the cylinders. The corresponding L_{uu} is 3.3, less than that (4.2) without the oscillation. The upstream cylinder oscillation changes the flow regime; the shear layers separating from the upstream cylinder reattach on, instead of shooting over, the downstream cylinder (Fig. 4(b)). Flow behind the cylinders is less spanwise-correlated in the reattachment regime than in the 'shooting over' regime (Table 1). On the other hand, the spanwise correlation appears improved, albeit slightly, at $L/d = 2.5$ and 4.8. Without changing the flow regime, the oscillation does enhance the spanwise correlation of flow behind the upstream cylinder, and subsequently the flow behind the downstream cylinder. The observation suggests that the two-dimensionality of the wake behind the downstream cylinder depends on the flow regime of the two cylinders, which is dependent on L/d, and the spanwise correlation of the flow between the cylinders.

3.3. Flow structure and predominant frequencies of flow structures

Fig. 4 shows flow at $L/d = 1.8$ measured using the visualization function of the PIV. When the upstream cylinder is stationary, the shear layers separating from the upstream cylinder appear to overshoot the downstream cylinder and the vortex street occurs only behind the cylinders. The end effect is discernible in the power spectral density function, E_u (Fig. 5), measured from the mid-span of the cylinder to the free end. The pronounced peak at $f^* = fd/U_\infty = 0.176$ is identified with the shear layer roll-up frequency, as confirmed by comparing with Xu and Zhou's (2004) measurement of the dominant frequencies in the flow around two tandem cylinders for the present L/d and Re. Unless otherwise stated,

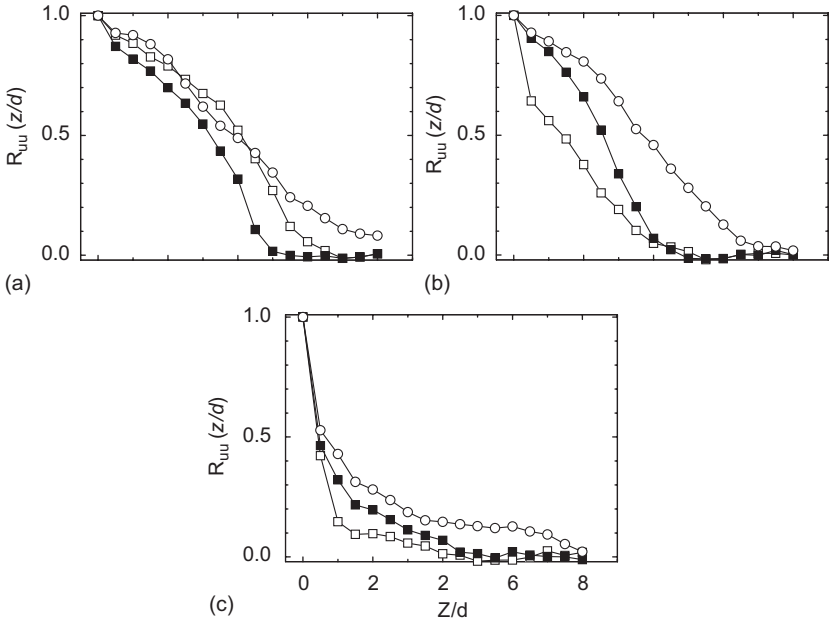

Fig. 3. Span-wise correlation coefficient, R_{uu}, of hotwire signals measured behind the cylinders at Re = 5920: (a) $L/d = 1.8$, (b) 2.5, and (c) 4.8. ■, Oscillation; □, without oscillation; ○, stationary cylinder with large-aspect-ratio of 47.

the superscript of asterisk denotes normalization by U_∞ and/or d in this paper. Another peak at $f^* = 2 \times 0.176$ is also discernible around $z^* = 0$. The peak at $f^* = 0.176$ gradually diminishes towards the free end, suggesting that the end effect acts to suppress the shear layer roll-up. Under the end effects, the spanwise coherence of the flow near the upstream cylinder impairs considerably, compared with that of the 'long' cylinders (Fig. 2(a)). However, the spanwise coherence of the flow is markedly improved behind the downstream cylinder (see Fig. 3(a)). Similar observations were made by Arie et al. (1983) and Igarashi (1980). The difference in L_{uu} between flows in the gap of and behind the cylinders is because the roll-up shear layer (vortex shedding) behind the downstream cylinder is inherently better correlated than the separating shear layer between the cylinders. Note that the peak at $f^* = 0.176$ in E_u between the cylinders is not necessarily due to vortex shedding from the upstream cylinder; instead, it probably results from the upstream feedback of vortex shedding from the downstream cylinder (Xu and Zhou, 2004).

In the presence of the upstream cylinder oscillation, the shear layer separating from the upstream cylinder appears to reattach to the downstream, instead of overshooting (Fig. 4(b)), that is, the flow regime changes from overshooting to reattachment. This change complicates the situation. On one hand, the improved two-dimensionality of incoming shear layer should correspond to an improved spanwise coherence around the downstream cylinder. On the other hand, the two-dimensionality of the flow around the downstream cylinder should lessen in the reattachment regime than in the overshooting regime. The combined effects lead to the deterioration of the flow two-dimensionality behind the downstream cylinder. The power spectral density function in Fig. 6(a) displays a peak at $f_e/f_s = 0.0372$ ($f_e^* = 0.00723$) between the cylinders. This peak remains pronounced even at $z/d = 12$, suggesting that the oscillation enhances greatly the two-dimensionality of flow near the upstream cylinder. Its harmonics up to $3f_e$ are discernible. Another peak, associated with natural vortex shedding occurs at $f^* = 0.171$, is slightly lower than without oscillation. The peak associated with the oscillation frequency remains pronounced behind the downstream cylinder (Fig. 6(b)). Natural vortex shedding diminishes for large z/d, implying the enhanced three-dimensionality of flow. The observation is consistent with the measured R_{uu} (Fig. 3(a)).

It is worth commenting on a possible connection between the shear layer vortices, being more responsive to the applied disturbance and the flow spanwise correlation in the gap of the cylinders. The u-spectrum in Fig. 5(a) ($L/d = 1.8$) displays a pronounced peak at $f^* = 0.176$ for $z/d < 8$, suggesting the presence of the shear layer vortices. Accordingly, there is a strong spanwise correlation in the gap of the cylinders (Fig. 2(a)). Once the oscillation is introduced, however, another pronounced peak occurs at f_e^* and the peak at $f^* = 0.171$ corresponding to the shear layer vortices between the cylinders becomes rather broadened (Fig. 6(a)), indicating that the shear layer vortices are quite responsive to the oscillation. Consequently, R_{uu} (Fig. 3(a)) drops appreciably. The observation points to a close link between the shear layer vortices and flow spanwise correlation.

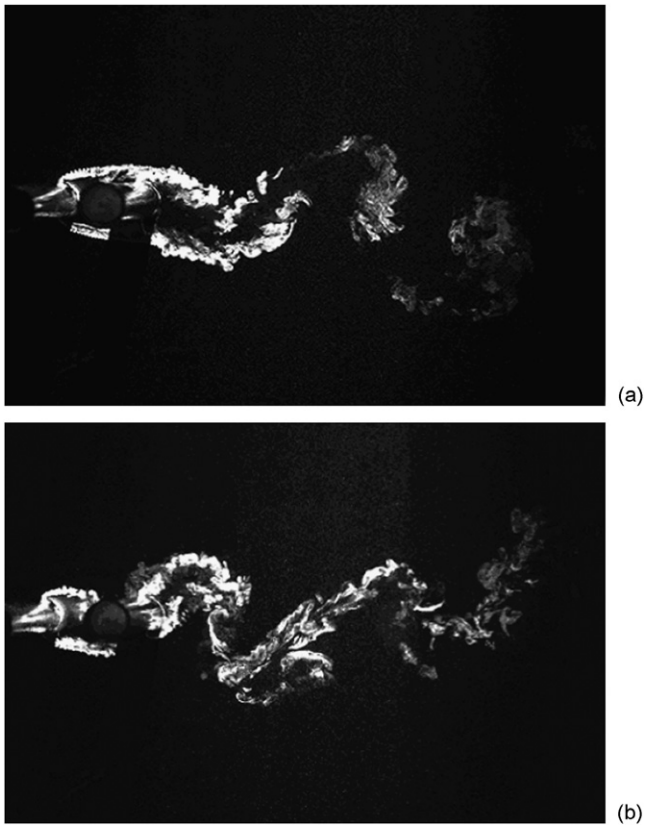

Fig. 4. Photograph of flow regime at $L/d = 1.8$: (a) without cylinder oscillation and (b) with cylinder oscillation.

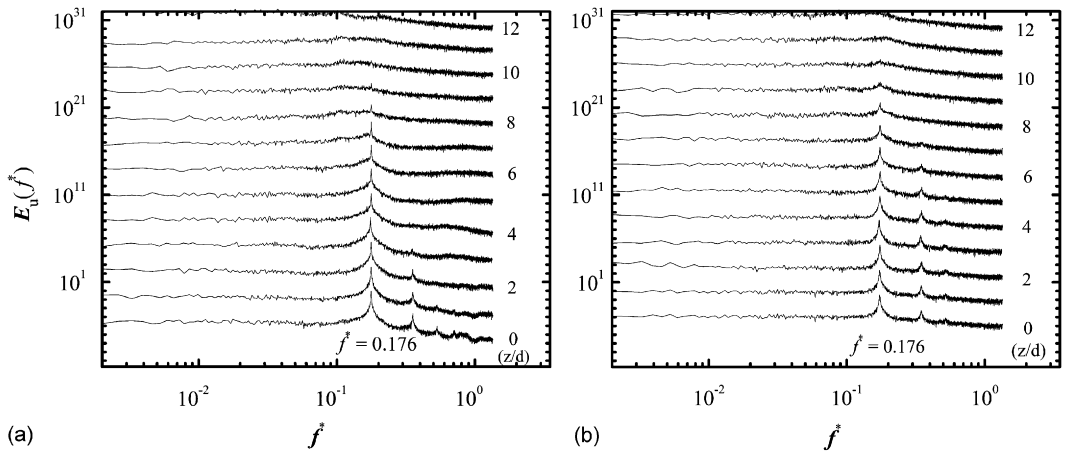

Fig. 5. Power spectral density function in the absence of cylinder vibration at $L/d = 1.8$: (a) between the cylinders and (b) behind the cylinders.

At $L/d = 2.5$, the shear layers separating from the upstream cylinder reattach on the downstream cylinder in the absence of the upstream cylinder oscillation (Fig. 7(a)). The impingement of the reattaching shear layers on the downstream cylinder, especially at the free ends, may act to weaken the spanwise coherence of vortices formed behind the downstream cylinder. This could explain why the flow between the cylinders is better spanwise-correlated than that behind the downstream cylinder (Figs. 2(b), 3(b)). Once the upstream cylinder oscillates, vortices are formed in the gap of the two cylinders as well as behind. The two-dimensionality of flow between the cylinders is enhanced because vortex

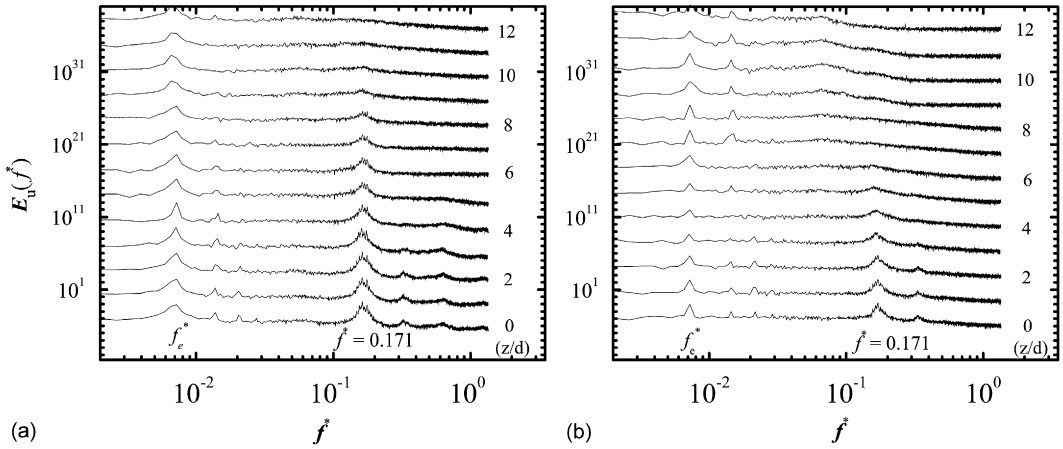

Fig. 6. Power spectral density function in the presence of cylinder vibration at $L/d = 1.8$: (a) between the cylinders and (b) behind the cylinders.

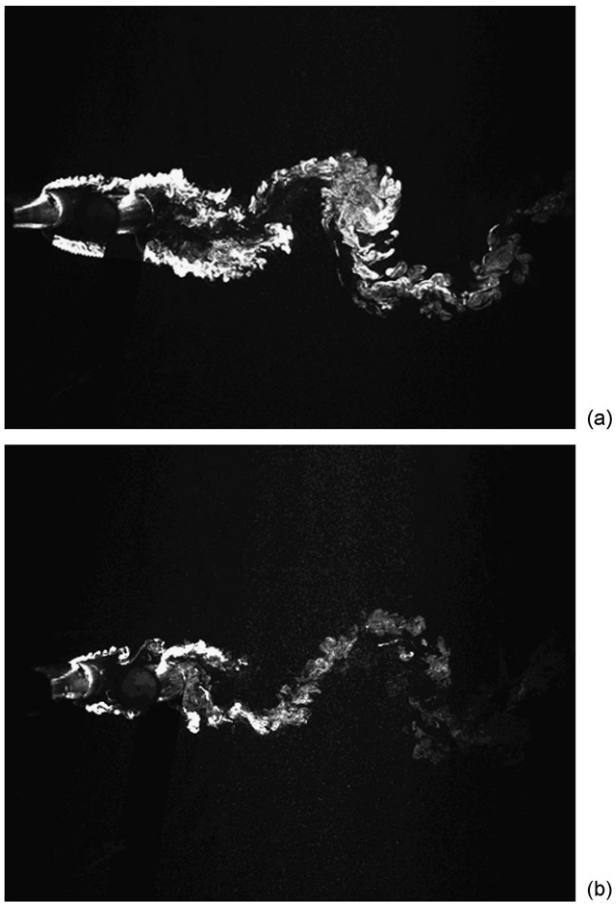

Fig. 7. Photograph of flow regime at $L/d = 2.5$: (a) without cylinder oscillation and (b) with cylinder oscillation.

shedding from the upstream cylinder occurs, which is locked on with the oscillation. This is evident in E_u (Fig. 9(a)), where only peaks at f_e and its harmonics are identifiable. These peaks are also discernible in E_u for the flow behind the downstream cylinder. Figs. 8 and 9 present the power spectra obtained from hotwire data for $L/d = 2.5$ with and

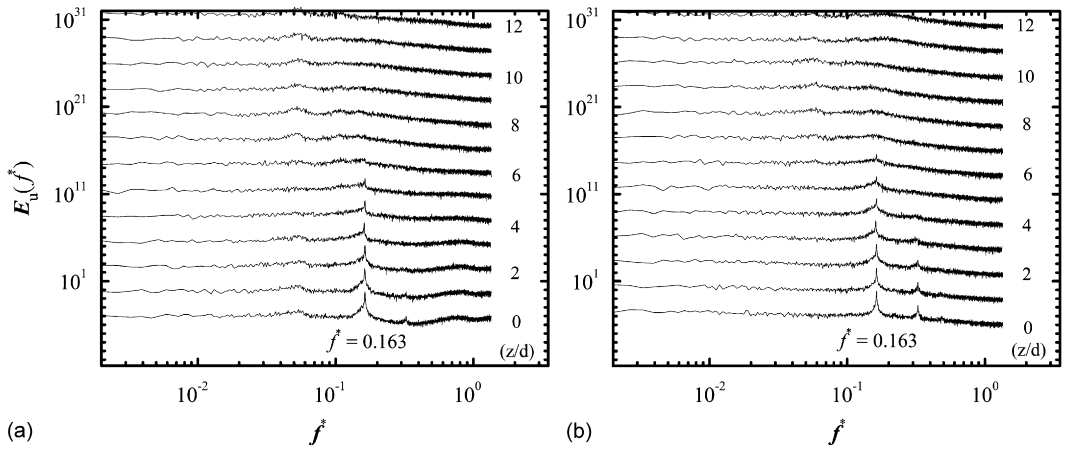

Fig. 8. Power spectral density function in the absence of cylinder vibration measured at $L/d = 2.5$: (a) between the cylinders and (b) behind the cylinders.

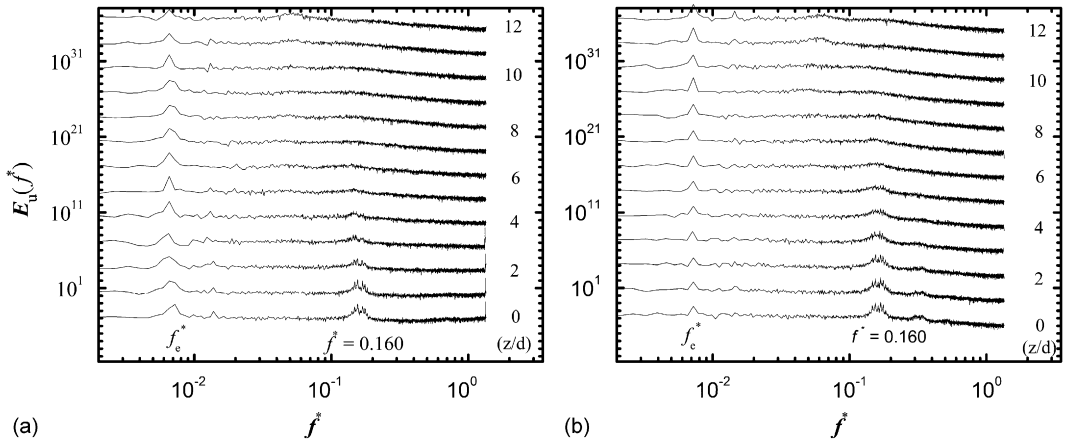

Fig. 9. Power spectral density function in the presence of cylinder vibration at $L/d = 2.5$: (a) between the cylinders and (b) behind the cylinders.

without the oscillation of the upstream cylinder, respectively. A pronounced peak occurs at $f^* = 0.163$ near the mid-span of the cylinder (Fig. 8(a)). Xu and Zhou (2004) noted that there could be a dominant frequency associated with the shear layers separating from the upstream cylinder in the reattachment regime. This peak at $f^* = 0.163$ is due to this dominant frequency of the shear layer separating from the upstream cylinder, as confirmed by comparing with the data of comparable Re and L/d in Xu and Zhou (2004). Another minor peak occurs at $f^* = 0.054 \approx 1/3 \times 0.163$, resulting from the nonlinearity of flow (Nayfeh and Mook, 1979). A pronounced peak occurs at $f^* = 0.163$ in Fig. 8(b), which is the dominant vortex frequency behind the downstream cylinder. When the oscillation is present, vortices are formed between the cylinders (Fig. 7(b)) and their frequency is locked on with the oscillation frequency (Xu and Zhou, 2005), as confirmed by the pronounced peak at $f_e^* = 0.00723$ (Fig. 9(a)). The peak at $f^* = 0.160$ that occurred in the absence of oscillation (Fig. 8(a)) is weakened. This is more evident towards the free end. A similar observation is made behind the downstream cylinder (Fig. 9(b)). As a consequence, there is a decreased spanwise correlation behind the cylinders, as observed in Fig. 3(b).

At $L/d = 4.8$, both cylinders appear shedding vortices (Fig. 10(a)). The spanwise correlation length of the flow is very small behind either of the cylinders (Fig. 2(c)), because of a strong three-dimensionality of spanwise vortices in the co-shedding regime (Zhou and Yiu, 2006). Once the oscillation is introduced, vortex shedding from the upstream cylinder is locked on with the oscillation and appears enhanced (Fig. 10(b)), resulting in increased spanwise coherence of the flow in the gap of the cylinders. However, the oscillation has a negligible effect on the spanwise coherence of the flow behind the downstream cylinder. In the absence of oscillation, a broad peak occurs at $f^* = 0.140$ between and

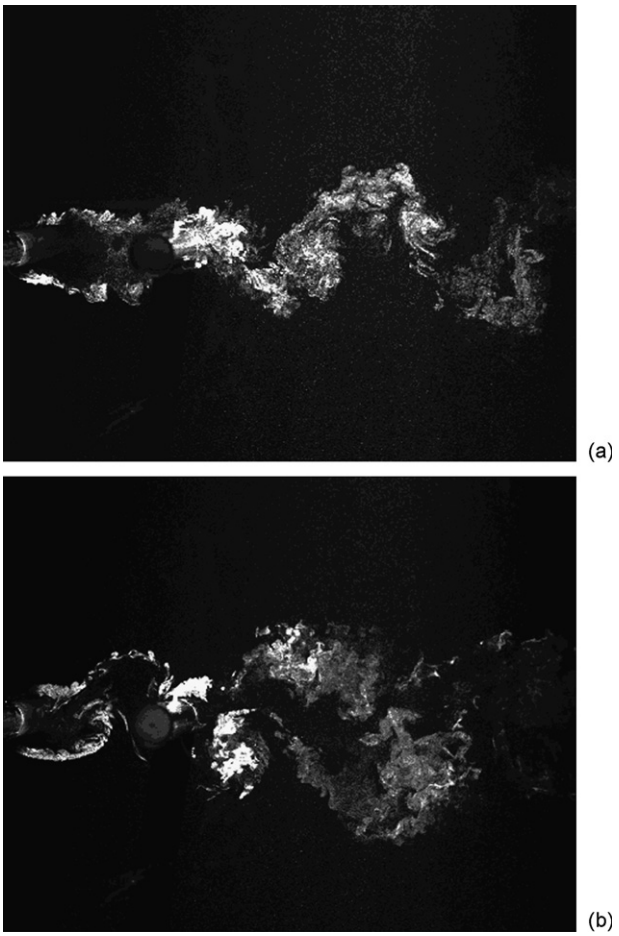

Fig. 10. Photograph of flow regime at $L/d = 4.8$: (a) without cylinder oscillation and (b) with cylinder oscillation.

behind the cylinders (Fig. 11). The end effect significantly decreases the two-dimensionality of flow, irrespective of being between and behind the cylinders, partially contributing to the broadness of the peak. When the upstream cylinder oscillation is introduced, a peak occurs at f_e*, which appears to have a negligibly small effect on the vortex shedding frequency (Fig. 12) but improving spanwise coherence, though only slightly (Figs. 2(c) and 3(c)).

4. Theoretical considerations

Experimental data (Section 3) indicate that R_{uu} depends on L/d, oscillation and end effects for 'short' cylinders. In this section, we attempt to understand more thoroughly the experimental observations.

Fig. 13(a) shows the sketch of an oscillating plate in a still fluid. This is a Stokes–Reyleigh problem, whose analytical solution is given in many textbooks [e.g., Wu et al. (2006)]. Based on the solution, a viscous oscillating wave in the boundary layer propagates away from the wall. The end of the oscillating cylinder may be approximately considered to be a moving surface in a steady flow. The wave velocity is roughly a combination of the free-stream velocity and that the surface would generate in still fluid (Fig. 13(b)). While propagating from the cylinder end, this wave acts to carry fluid particles away from the cylinder end, thus impairing the end effect. Since the cylinder oscillation enhances the vorticity component ω_z around the oscillating cylinder (Xu et al., 2006), the other two components, ω_x and ω_y, become relatively weak. The coherence of vorticity along the spanwise direction is linked with the two-dimensionality of flow; given $\omega_z \gg \omega_x$ or ω_y, the flow is predominantly 2-D.

It may be insightful into the physics behind the experimental observations to examine vorticity generated from the cylinder surface. For incompressible flow, the 3-D vorticity flux σ on the surface of the cylinder is given by

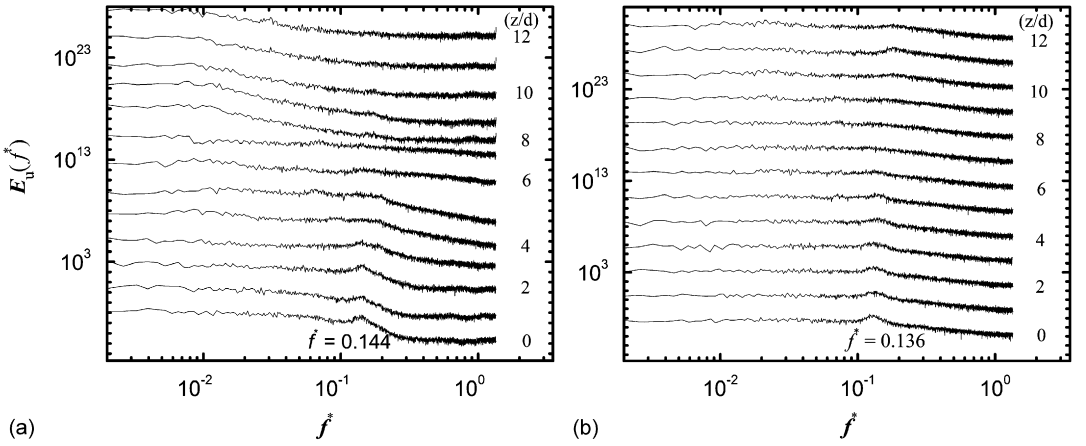

Fig. 11. Power spectral density function in the absence of cylinder vibration at $L/d = 4.8$: (a) between the cylinders and (b) behind the cylinders.

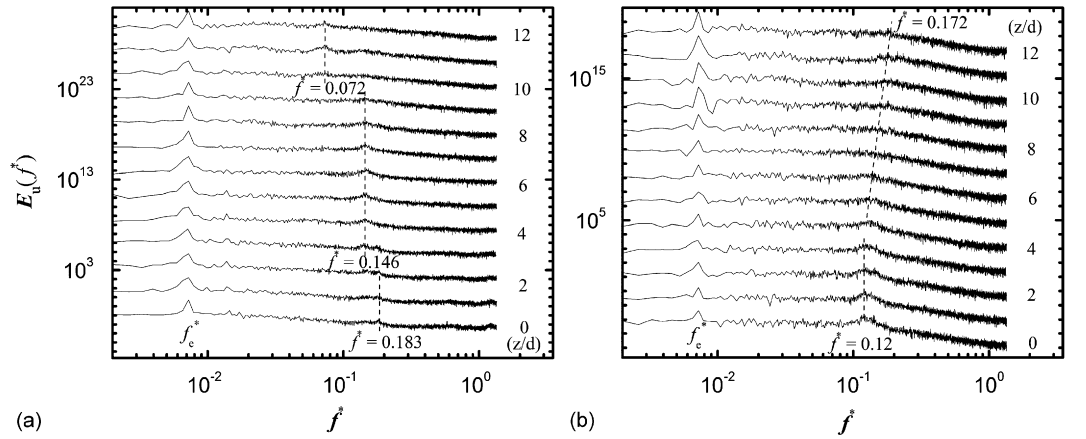

Fig. 12. Power spectral density function in the presence of cylinder vibration at $L/d = 4.8$: (a) between the cylinders and (b) behind the cylinders.

(Wu and Wu, 1993)

$$\boldsymbol{\sigma} = -\nu \boldsymbol{n} \cdot \nabla \boldsymbol{\omega} = -\boldsymbol{n} \times (\nabla p + \rho \boldsymbol{a}) - (\boldsymbol{n} \times \nabla) \cdot (\nu \boldsymbol{\omega} \times \boldsymbol{nn}), \tag{2}$$

where $\boldsymbol{n}$ is the unit vector pointing outward normal to the cylinder surface, p is the pressure, $\boldsymbol{a}$ is the acceleration of the cylinder, $\boldsymbol{\omega}$ is the vorticity vector, and ρ is the density of fluid. All terms in Eq. (2) are evaluated on the cylinder surface. The vorticity flux $\boldsymbol{\sigma}$ represents the changing rate of the vortex source strength over a unit area of the cylinder surface, representing the distribution of vorticity in different directions. Assume the cylinder oscillation to be described by

$$X(t) = A\cos(2\pi f_e t + \varphi_0), \tag{3}$$

where φ_0 is the initial phase angle of the oscillating cylinder. Then the cylinder acceleration is

$$a = \ddot{X}(t) = -4\pi^2 f_e^2 A\cos(2\pi f_e t + \varphi_0). \tag{4}$$

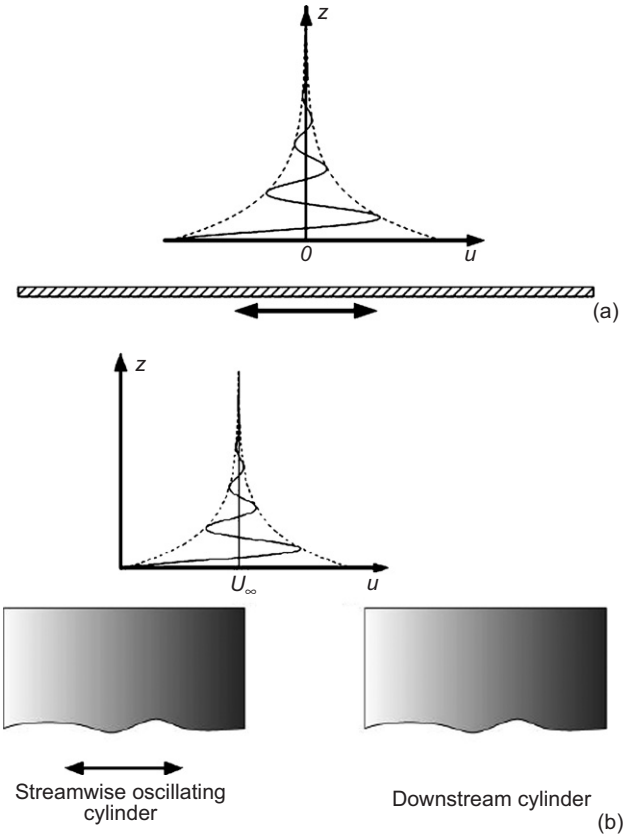

Fig. 13. Stokes layer of (a) a moving wall and (b) at the end of the oscillating cylinder.

In a moving cylindrical coordinate system (r, θ, z), fixed on the upstream cylinder, σ may be rewritten as

$$\begin{Bmatrix} \sigma_r \\ \sigma_\theta \\ \sigma_z \end{Bmatrix} = \begin{Bmatrix} -v\dfrac{\partial \omega_r}{\partial r} \\ -v\dfrac{\partial \omega_\theta}{\partial r} \\ -v\dfrac{\partial \omega_z}{\partial r} \end{Bmatrix} = \begin{Bmatrix} -v\left(\dfrac{1}{r_0}\dfrac{\partial \omega_z}{\partial \theta} + \dfrac{\partial \omega_\theta}{\partial z}\right) \\ -\left(\dfrac{\partial p(\theta, z, t)}{\partial z} + v\dfrac{\omega_z}{r_0}\right) \\ -\dfrac{1}{r_0}\dfrac{\partial p(\theta, z, t)}{\partial \theta} + 4\pi^2 f_e^2 A\rho\cos(2\pi f_e t + \varphi_0)\sin\theta \end{Bmatrix}, \tag{5}$$

where r_0 is the cylinder radius. Based on Eq. (5), the cylinder oscillation ($f_e \neq 0$ and $A \neq 0$) increases σ_z. The other two components σ_r and σ_θ, multiplied by the kinematic viscosity, are small compared with σ_z. This could explain why R_{uu} can be enhanced by oscillation. When f_e/f_s is increased from 0.0372 to $0.0372 \times 5 = 0.186$, L_{uu} between the cylinders is increased from 5.2 to 6.5 for $L/d = 1.8$, and from 3.5 to 4.6 for $L/d = 2.5$ (not shown), up to 25% for both L/d, conforming to the prediction from Eq. (5).

The acceleration term in Eq. (5) vanishes for the downstream cylinder, viz.,

$$\begin{Bmatrix} \sigma_r \\ \sigma_\theta \\ \sigma_z \end{Bmatrix} = \begin{Bmatrix} -v\dfrac{\partial \omega_r}{\partial r} \\ -v\dfrac{\partial \omega_\theta}{\partial r} \\ -v\dfrac{\partial \omega_z}{\partial r} \end{Bmatrix} = \begin{Bmatrix} -v\left(\dfrac{1}{r_0}\dfrac{\partial \omega_z}{\partial \theta} + \dfrac{\partial \omega_\theta}{\partial z}\right) \\ -\left(\dfrac{\partial p(\theta, z, t)}{\partial z} + v\dfrac{\omega_z}{r_0}\right) \\ -\dfrac{1}{r_0}\dfrac{\partial p(\theta, z, t)}{\partial \theta} \end{Bmatrix}. \tag{6}$$

Based on Eq. (6) the oscillation has no direct effect on flow around the downstream cylinder, and the voriticy flux around the downstream cylinder remains to be governed by the absolute stability of flow, i.e., the pressure gradient around the cylinder, which largely depends on the flow regime. The result conforms to measurements shown in Fig. 3.

5. Conclusions

The effect of a longitudinally oscillating cylinder on the two-dimensionality of a downstream cylinder wake has been investigated. The aspect ratio of the cylinders is 17. The oscillating amplitude was $A/d = 0.472$ and the oscillation frequency was $f_e/f_s = 0.0372$ and 0.186. The two-dimensionality of the flow around the cylinders is dependent on aspect ratio, flow regimes and cylinder oscillation. The following conclusions may be drawn.

(i) The two-dimensionality of flow depends on the flow regime. Without cylinder oscillation, the flow two-dimensionality between the cylinders is worst in the 'single-body' regime, but improved in the reattachment and the co-shedding regimes; in the case of the 'long' cylinders L_{uu} is 3.0, 4.2 and 4.3 at $L/d = 1.8$, 2.5 and 4.8, respectively. The flow two-dimensionality behind the cylinders is improved appreciably in the 'single-body' regime but worsens greatly in the co-shedding regime; the corresponding L_{uu} is 4.0, 3.8 and 0.8 for the three regimes. For 'short' cylinders, as expected, the flow two-dimensionality worsens because of the end effects in the reattachment and the co-shedding regimes, irrespective of between and behind the cylinders. However, this two-dimensionality is improved behind the cylinders in the 'single-body' regime, with L_{uu} at $L/d = 1.8$ increasing by 91%, compared with that between the 'short' cylinders; L_{uu} is, in fact, comparable with that in the case of 'long' cylinders. The observation suggests a negligible end effect in the 'single-body' regime.

(ii) The cylinder oscillation enhances greatly the two-dimensionality of the flow between the cylinders in all regimes. In the absence of the oscillation, L_{uu} is 2.2, 1.6 and 0.4 between the 'short' cylinders at $L/d = 1.8$, 2.5 and 4.8, respectively; with the upstream cylinder oscillating, it increases by 137%, 119% and 50%, respectively. Two factors contribute to the enhanced two-dimensionality of flow between the cylinders: (a) theoretical analysis indicates that the cylinder oscillation promotes directly the generation of the spanwise vorticity (ω_z) near the oscillating cylinder; and (b) the cylinder oscillation generates a wave at the end, which carries away fluid particles, thus decreasing significantly the end effect (Fig. 13(b)).

(iii) The cylinder oscillation has a negligibly small effect on the two-dimensionality of flow behind the cylinders; neither the generation of ω_z nor the cylinder oscillation effect on the flow near the downstream cylinder end is significant.

Acknowledgements

SJX acknowledges the funding support by NSFC through Grant 10642002. YZ wishes to acknowledge support given to him by the Research Grants Council of the Government of the HKSAR through Grants PolyU 5316/03E. JYT is grateful for the financial support of Australian Research Council through Projects ARC-DP055094 and ARC-SR0563610. The authors acknowledge Mr J. F. Huang's and Dr G. Xu's contributions to the experimental work.

References

Arie, M., Kiya, M., Moriya, M., Mori, H., 1983. Pressure fluctuations on the surface of two circular cylinders in tandem arrangement. ASME Journal of Fluids Engineering 105, 161–167.

Bishop, R.E.D., Hassan, A.Y., 1964. The lift and drag forces on a circular cylinder oscillating in a flowing fluid. Proceedings of the Royal Society (London) Series A 277, 51–59.

Blackburn, H.M., Melbourne, W.H., 1997. Sectional lift forces for an oscillating circular cylinder in smooth and turbulent flows. Journal of Fluids and Structures 11, 413–431.

Griffin, O.M., 1980. OTEC cold water pipe design for problems caused by vortex-excited oscillation. NRL Memorandum Report 4157, Naval Research Laboratory, Washington, DC.

Huang, J.F., Zhou, Y., Zhou, T.M., 2006. Three-dimensional wake structure measurement using a modified PIV technique. Experiments in Fluids 40, 884–896.

Igarashi, T., 1981. Characteristics of the flow around two circular cylinders arrangement in tandem (1st report). Bulletin of the JSME 24, 323–331.

King, R., 1977. A review of vortex shedding research and its application. Ocean Engineering 4, 141–171.

Koopmann, G.H., 1967. The vortex wakes of vibrating cylinders at low Reynolds numbers. Journal of Fluid Mechanics 28, 501–512.
Lai, W.C., Zhou, Y., So, R.M.C., Wang, T., 2003. Interference between a stationary and a vibrating cylinder wake. Physics of Fluids 15, 1687–1695.
Lucor, D., Foo, J., Karniadakis, G.E., 2003. Correlation length and force phasing of rigid cylinder subject to VIV. In: IUTAM Symposium, June 2003, New Brunswick, New Jersey, USA.
Mahir, N., Rockwell, D., 1996a. Vortex formation from a forced system of two cylinders: part I: tandem arrangement. Journal of Fluids and Structures 10, 473–489.
Mahir, N., Rockwell, D., 1996b. Vortex formation from a forced system of two cylinders: part II: side-by-side arrangement. Journal of Fluids and Structures 10, 491–500.
Nayfeh, A.H., Mook, D.T., 1979. Nonlinear Oscillations. Wiley, New York, p. 139.
Norberg, C., 2003. Fluctuating lift on a circular cylinder: review and new measurements. Journal of Fluids and Structures 17, 57–96.
Ramberg, S.E., Griffin, O.M., 1976. Velocity correlation and vortex spacing in the wake of a vibrating cable. ASME Journal of Fluids Engineering 98, 10–18.
Ribeiro, J.D., 1992. Fluctuating lift and its spanwise correlation on a circular cylinder in a smooth and a turbulent flow: a critical review. Journal of Wind Engineering and Industrial Aerodynamics 40, 179–198.
Szepessy, S., 1994. On the spanwise correlation of vortex shedding from a circular cylinder at high subcritical Reynolds number. Physics of Fluids 6, 2406–2416.
Szepessy, S., Bearman, P.W., 1992. Aspect ratio and end plate effects on vortex shedding from a circular cylinder. Journal of Fluid Mechanics 234, 191–217.
Toebes, G.H., 1969. The unsteady flow and wake near an oscillating cylinder. ASME Journal of Basic Engineering 91, 493–505.
Wu, J.Z., Wu, J.M., 1993. Interactions between a solid-surface and a viscous compressible flow-field. Journal of Fluid Mechanics 254, 183–211.
Wu, J., Welch, L.W., Welsh, M.C., Sheridan, J., Walker, G.J., 1994. Spanwise wake structures of a circular cylinder and two circular cylinders in tandem. Experimental Thermal and Fluid Science 9, 299–308.
Wu, J.Z., Ma, H.Y., Zhou, M.D., 2006. Vorticity and Vortex Dynamics. Springer, USA, pp. 150–160.
Xu, G., Zhou, Y., 2004. Strouhal numbers in the wake of two inline cylinders. Experiments in Fluids 37, 248–256.
Xu, G., Zhou, Y., 2005. Momentum and heat transport in a turbulent cylinder wake behind a streamwise oscillating cylinder. International Journal of Heat and Mass Transfer 48, 4062–4072.
Xu, S.J., Zhou, Y., Wang, M.H., 2006. A symmetric binary vortex street behind a longitudinally oscillating cylinder. Journal of Fluid Mechanics 556, 27–43.
Zdravkovich, M.M., 1987. The effects of interference between circular cylinders in cross flow. Journal of Fluids and Structures 1, 239–261.
Zhou, Y., Antonia, R.A., 1995. Memory effects in a turbulent plane wake. Experiments in Fluids 19, 112–120.
Zhou, Y., Yiu, M.W., 2006. Flow structure, momentum and heat transport in a two-tandem-cylinder wake. Journal of Fluid Mechanics 548, 17–48.
Zhou, Y., Zhang, H.J., Yiu, M.W., 2002. The turbulent wake of two side-by-side circular cylinders. Journal of Fluid Mechanics 458, 303–332.